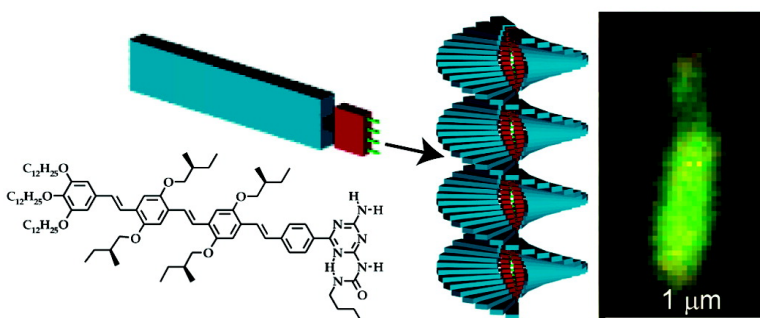


Polarized Emission of Individual Self-Assembled Oligo(*p*-phenylenevinylene)-Based Nanofibers on a Solid Support

Ccile R. L. P. N. Jeukens, Pascal Jonkheijm, Frans J. P. Wijnen, Jeroen C. Gielen, Peter C. M. Christianen, Albertus P. H. J. Schenning, E. W. Meijer, and Jan C. Maan

J. Am. Chem. Soc., **2005**, 127 (23), 8280-8281 • DOI: 10.1021/ja051781c • Publication Date (Web): 21 May 2005

Downloaded from <http://pubs.acs.org> on March 25, 2009



More About This Article

Additional resources and features associated with this article are available within the HTML version:

- Supporting Information
- Links to the 11 articles that cite this article, as of the time of this article download
- Access to high resolution figures
- Links to articles and content related to this article
- Copyright permission to reproduce figures and/or text from this article

[View the Full Text HTML](#)

Polarized Emission of Individual Self-Assembled Oligo(*p*-phenylenevinylene)-Based Nanofibers on a Solid Support

Cécile R. L. P. N. Jeukens,[†] Pascal Jonkheijm,[§] Frans J. P. Wijnen,[†] Jeroen C. Gielen,[†] Peter C. M. Christianen,^{*,†} Albertus P. H. J. Schenning,^{*,§} E. W. Meijer,[§] and Jan C. Maan[†]

High Field Magnet Laboratory, Institute for Molecules and Materials, Radboud University Nijmegen, Toernooiveld 7, 6525 ED Nijmegen, The Netherlands, and Laboratory of Macromolecular and Organic Chemistry, Eindhoven University of Technology, P.O. Box 513, 5600 MB Eindhoven, The Netherlands

Received March 21, 2005; E-mail: P.Christianen@science.ru.nl; A.P.H.J.Schenning@tue.nl

The development of nanofibers is a promising approach to miniaturize optoelectronic devices. Over the recent years, such fibers have been constructed from inorganic materials¹ and carbon nanotubes.² Alternatively, self-assembled³ nanofibers based on π -conjugated systems provide a versatile means to fabricate fibers with tailor-made functionalities similar to those of plastic electronics.^{4,5} So far, however, their use in devices has been limited to π -conjugated polymers and doped oligomers.^{6,7} A crucial step toward plastic nanoelectronics is the creation of identical, highly organized fibers, about one-molecule thick, on a solid support. Since the internal organization of such fibers determines their performance, it is important to develop techniques to structurally characterize *individual* fibers at the molecular level. Here, we employ polarized fluorescence microscopy (FM)^{8,9} on single oligo-(*p*-phenylenevinylene)-based fibers, deposited on a graphite surface. The fibers exhibit a profound polarized optical emission over their entire length that directly corresponds to their orientation on the substrate. The observed polarization ratio (~ 2) is rather low, but taking into account the dielectric constant of graphite and the helical nature of the fibers, the data reveal a high degree of internal order.

We recently reported the construction of stacks consisting of tetra(*p*-phenylenevinylene)-based molecules (OPV, Figure 1a,b).¹⁰ OPV dimers, formed via the self-complementary quadrupole ureido-s-triazine hydrogen bonding units (Figure 1c), self-assemble in cylindrical chiral stacks due to π - π interactions of the phenylenevinylene backbone (Figure 1d). In solution, these stacks have a cooperative length of 150 nm and a 5 nm diameter.

After transfer to a suitable solid support, such as graphite or silicon oxide, the fibers have the same diameter as in solution, but the length can reach up to several micrometers, presumably due to further end-to-end assembly of the stacks (Figure 1e,f).¹¹ So far, we could not prove whether the proposed internal organization of the fibers is correct and preserved on a solid support.

The dominant optical dipole moments for absorption and emission of the OPV building block are directed along the long axis of the tetra(*p*-phenylenevinylene) unit and are expected to be perpendicular to the fiber axis (Figure 1).¹² Such a molecular arrangement should result in a pronounced polarization of the fluorescence emission of a single fiber. Figure 2 depicts polarized fluorescence images¹³ of individual fibers. The emission spectrum of a single fiber on graphite is similar to that in solution.¹³ The FM pictures are constructed from two measurements. First, the fluorescence intensity I_{HOR} is measured with horizontal (0°) orientation of the excitation and detection polarizations with respect to the image (Figure 2a). Next, the fluorescence intensity I_{VER} is detected with the excitation and detection polarizations in the

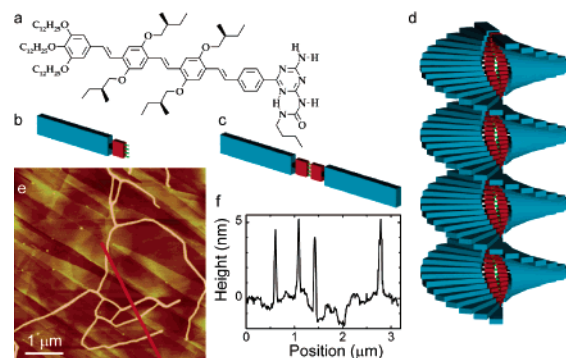


Figure 1. (a) Chemical structure of the OPV building block. Schematic representation of (b) OPV, (c) OPV dimer, and (d) helical stacks of OPV dimers at 12° with respect to each other. (e) AFM image of OPV fibers on graphite. (f) Cross section through several fibers (along red line in e).

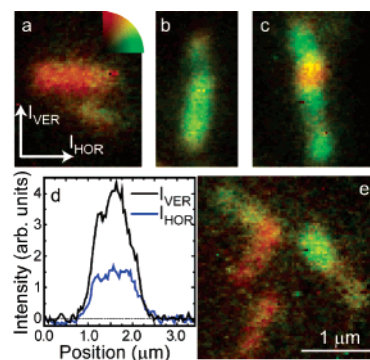


Figure 2. Real-space polarized FM images (a, b, c, e) of various OPV nanofibers on graphite. The color-coding (upper-right corner in a) corresponds to the intensity ratio of two consecutive measurements with horizontal (0° , I_{HOR}) and vertical polarization (90° , I_{VER}): $R = I_{\text{VER}}/I_{\text{HOR}}$ ranging from green ($R < 1$) to red ($R > 1$) through yellow ($R = 1$). The white arrows in a denote the orientation of the polarizers. (d) Profile of I_{VER} and I_{HOR} through the fiber shown in a.

vertical (90°) direction. The measurements lead to a value of the polarization ratio $R = I_{\text{VER}}/I_{\text{HOR}}$, which is expressed in the images as a color-coding, ranging from green ($R < 1$) to red ($R > 1$) through yellow ($R = 1$). The orientation of the fibers in the images is their true physical orientation with respect to the polarizers. In total, we have performed this extensive experimental analysis for 14 individual nanofibers, randomly oriented on the surface.

The images reveal that the fluorescence of each fiber is strongly polarized, with a direction that is correlated to its orientation on the surface. For example, Figure 2a shows a fiber of about $1 \mu\text{m}$ length, horizontally oriented, with a uniform red color, indicating that the fluorescence is vertically polarized over the entire fiber. The emission profile of this fiber (Figure 2d) shows that the

[†] Radboud University Nijmegen.

[§] Eindhoven University of Technology.

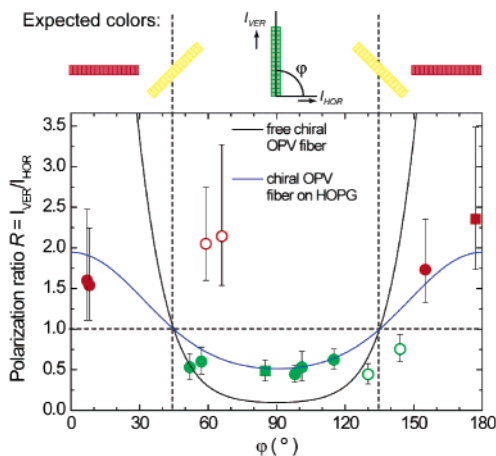


Figure 3. Measured polarization ratios R of 14 OPV nanofibers (symbols) as a function of their orientation φ . The color of the symbols reflects the color-coding of the measured R (red, $R > 1$; green, $R < 1$). The solid lines are calculations of R considering chiral OPV fibers (Figure 1d) in vacuum (black line) or on graphite (blue line). Top panel: the expected polarization degree and color-coding for chiral OPV fibers.

vertically polarized fluorescence intensity (black curve) is considerably higher than that of the horizontal polarization (blue curve), yielding a polarization ratio $R = 2.4$. In contrast, the vertically oriented fiber in Figure 2b, exhibits an overall green color, that is, a horizontal polarization of the fluorescence. The direct relationship between the light polarization and fiber orientation is also clear from Figure 2e, which shows three fibers, one of them having a 90° bend, leading to a change in the color-code at the intersection. Most of the self-assembled fibers reveal a uniform polarization over micrometer ranges, due to effective head-to-tail positioning of the smaller stacks in solution, and only few of them are not polarized uniformly. For instance, the color-coded image of the long vertical fiber in Figure 2c displays a red defect in the overall green fiber, which indicates the mispositioning of one stack with respect to the others.

Figure 3 shows the average polarization ratio R of all 14 fibers as a function of the angle φ of the fiber direction with the horizontal axis. For clarity, the data points are given the same color as the color-coding corresponding to the experimentally observed fluorescence polarization, that is, red ($R > 1$) or green ($R < 1$). For example, the red and green closed squares represent the fibers in Figure 2a and b, respectively. On the basis of the quantitative results in Figure 3, two important conclusions can be drawn. First, 10 out of 14 fibers indeed show the color-coding expected for well-ordered nanofibers with the constituting dimers, arranged perpendicularly to the fiber axis (top panel Figure 3). Namely, nanofibers with $45^\circ < \varphi < 135^\circ$ appear green in this graph, whereas the others ($0^\circ < \varphi < 45^\circ$ or $135^\circ < \varphi < 180^\circ$) are red. Only four of the measured fibers show an unexpected color-coding (open circles in Figure 3), revealing a different orientation of the OPV dimers in the fibers. It is striking that these four fibers were situated in one region of the substrate (Figure 2e), and remarkably, the orientation of the OPV is the same in these four cases. These deviations possibly result from a locally different surface area that changes the molecule–surface interactions.¹¹ The second conclusion is that, although all fibers exhibit a profound polarization, the maximum polarization ratio is rather low ($R \approx 2$), in seeming contrast with a high degree

of order within the nanofibers. To explain this observation, we have calculated R as a function of fiber orientation, using a model that determines the polarized optical response of a chiral fiber (Figure 1d) by summing up the constituent optical dipoles.^{8,13} The model takes into account depolarizing effects of both the FM setup and the graphite substrate,¹³ but does not include any fit parameters. The result of this calculation (blue line in Figure 3) describes the observed data remarkably well. From our model, we find that there are two main reasons for the rather low polarization degree. First, the chiral composition of the stacks implies that the emission is the sum of polarized and *unpolarized* contributions of horizontal and vertical dipoles, respectively.¹³ This unpolarizing effect of the vertical dipoles alone is, however, not sufficient to explain our data (Figure 3, black curve, calculated for free chiral OPV stacks). Second, the complex dielectric constant of the underlying graphite results in a lower intensity of the polarized horizontal dipoles as compared to that of the unpolarized vertical dipoles, which causes a drastic reduction of R .¹³ The polarization degree of ideal chiral OPV fibers on graphite is, therefore, theoretically limited to $R \approx 2$, which is in excellent agreement with our FM results.

In conclusion, we have prepared 5 nm diameter, micrometer long OPV fibers on a surface that show a profound polarized optical emission. Our results show the high degree of organization within chiral fibers, with the OPV dimers oriented perpendicularly to the fiber axis. The control of the internal order within self-assembled fibers, and the ability to measure it, is a crucial step to obtain uniform organic fibers that can be applied in nanosized electronics at room temperature.

Acknowledgment. We thank Dr. S. De Feyter and Prof. N. F. van Hulst for valuable discussions. This work is part of the research programs of the “Stichting voor Fundamenteel Onderzoek der Materie (FOM)”, and the Council for the Chemical Sciences (CW), financially supported by the Dutch Organization for Scientific Research (NWO).

Supporting Information Available: Detailed experimental procedures and calculations. This material is available free of charge via the Internet at <http://pubs.acs.org>.

References

- (1) For a review: Xia, Y.; Yang, P.; Sun, Y.; Wu, Y.; Mayers, B.; Gates, B.; Yin, Y.; Kim, F.; Yan, H. *Adv. Mater.* **2003**, *15*, 353.
- (2) For a review: *Acc. Chem. Res.* **2002**, *35*, issue 12.
- (3) Lehn, J.-M. *Supramolecular Chemistry: Concepts and Perspectives*; VCH: New York, 1995.
- (4) Forrest, S. R. *Nature* **2004**, *428*, 911.
- (5) Hoeben, F. J. M.; Jonkheijm, P.; Meijer, E. W.; Schenning, A. P. H. J. *Chem. Rev.* **2005**, *105*, 1491.
- (6) (a) Merlo, J. A.; Frisbie, C. D. *J. Polym. Sci. B* **2003**, *41*, 2674 (b) Mas-Torrent, M.; den Boer, D.; Durkut, M.; Hadley, P.; Schenning, A. P. H. *J. Nanotechnology* **2004**, *15*, 265.
- (7) (a) Hill, J. P.; Jin, W.; Kosaka, A.; Fukushima, T.; Ichihara, H.; Shimomura, T.; Ito, K.; Hashizume, T.; Ishii, N.; Aida, T. *Science*, **2004**, *304*, 1841. (b) Messmore, B. W.; Hulvat, J. F.; Sone, E. D.; Stupp, S. I. *J. Am. Chem. Soc.* **2004**, *126*, 14452.
- (8) Jeukens, C. R. L. P. N.; Lensen, M. C.; Wijnen, F. J. P.; Elemans, J. A. A. W.; Christianen, P. C. M.; Rowan, A. E.; Gerritsen, J. W.; Nolte, R. J. M.; Maan, J. C. *Nano Lett.* **2004**, *4*, 1401.
- (9) Yan, P.; Chowdhury, A.; Holman, M. W.; Adams, D. M. *J. Phys. Chem B* **2005**, *109*, 724.
- (10) Schenning, A. P. H. J.; Jonkheijm, P.; Peeters, E.; Meijer, E. W. *J. Am. Chem. Soc.* **2001**, *123*, 409.
- (11) Jonkheijm, P.; Hoeben, F. J. M.; Kleppinger, R.; Van Herikhuyzen, J.; Schenning, A. P. H. J.; Meijer, E. W. *J. Am. Chem. Soc.* **2003**, *125*, 15941.
- (12) Spano, F. C. *J. Chem. Phys.* **2002**, *116*, 5877.
- (13) See Supporting Information.

JA051781C